Bioorganic & Medicinal Chemistry Letters 22 (2012) 527–531

Contents lists available at SciVerse ScienceDirect

Bioorganic & Medicinal Chemistry Letters

journal homepage: www.elsevier.com/locate/bmcl

Quinolinone-based agonists of $S1P_1$: Use of a N-scan SAR strategy to optimize in vitro and in vivo activity

Lewis D. Pennington [a,*], Michael D. Croghan [a], Kelvin K.C. Sham [a], Alexander J. Pickrell [a], Paul E. Harrington [a], Michael J. Frohn [a], Brian A. Lanman [a], Anthony B. Reed [a], Matthew R. Lee [b], Han Xu [c], Michele McElvain [c], Yang Xu [d], Xuxia Zhang [e], Michael Fiorino [e], Michelle Horner [f], Henry G. Morrison [g], Heather A. Arnett [e], Christopher Fotsch [a], Andrew S. Tasker [a], Min Wong [e], Victor J. Cee [a]

[a] Medicinal Chemistry, Amgen, One Amgen Center Drive, Thousand Oaks, CA 91320, USA
[b] Molecular Structure, Amgen, One Amgen Center Drive, Thousand Oaks, CA 91320, USA
[c] HTS and Molecular Pharmacology, Amgen, One Amgen Center Drive, Thousand Oaks, CA 91320, USA
[d] Pharmacokinetics and Drug Metabolism, Amgen, One Amgen Center Drive, Thousand Oaks, CA 91320, USA
[e] Inflammation Research, Amgen, One Amgen Center Drive, Thousand Oaks, CA 91320, USA
[f] Toxicology, Amgen, One Amgen Center Drive, Thousand Oaks, CA 91320, USA
[g] Pharmaceutics, Amgen, One Amgen Center Drive, Thousand Oaks, CA 91320, USA

ARTICLE INFO

Article history:
Received 4 October 2011
Revised 24 October 2011
Accepted 26 October 2011
Available online 4 November 2011

Keywords:
Sphingosine-1-phosphate-1 receptor agonist
Physicochemical properties
Immunosuppression
Multiple sclerosis
N-scan SAR

ABSTRACT

We reveal how a N-scan SAR strategy (systematic substitution of each CH group with a N atom) was employed for quinolinone-based $S1P_1$ agonist **5** to modulate physicochemical properties and optimize in vitro and in vivo activity. The diaza-analog **17** displays improved potency (h$S1P_1$ RI; **17**: EC_{50} = 0.020 μM, 120% efficacy; **5**: EC_{50} = 0.070 μM, 110% efficacy) and selectivity (h$S1P_3$ Ca^{2+} flux; **17**: EC_{50} >25 μM; **5**: EC_{50} = 1.5 μM, 92% efficacy), as well as enhanced pharmacokinetics (**17**: CL = 0.15 L/h/kg, V_{dss} = 5.1 L/kg, $T_{1/2}$ = 24 h, %*F* = 110; **5**: CL = 0.93 L/h/kg, V_{dss} = 11 L/kg, $T_{1/2}$ = 15 h, %*F* = 60) and pharmacodynamics (**17**: 1.0 mg/kg po, 24 h PLC POC = −67%; **5**: 3 mg/kg po, 24 h PLC POC = −51%) in rat.

Sphingosine-1-phosphate (**1**, S1P) is the endogenous ligand for the G-protein-coupled receptors $S1P_{1-5}$ and participates in modulating a wide variety of physiological processes including cell motility, pulmonary endothelium integrity, and cardiovascular function (Fig. 1).[1] S1P (**1**) and the sphingosine-1-phosphate-1 receptor ($S1P_1$) were discovered several years ago to regulate the trafficking of lymphocytes from the lymphatic system.[2] Exposure to high concentrations of **1** or synthetic agonists of $S1P_1$ induces receptor internalization (RI) of $S1P_1$ located on the cell surface of lymphocytes in lymphatic tissues and prevents lymphocyte egress to the systemic circulation and central nervous system (**1**: h$S1P_1$ RI EC_{50} = 0.018 μM, 91% efficacy).[3,4] Synthetic agonists of $S1P_1$ are being investigated intensely as potential immunosuppressive therapies for a variety of conditions, including multiple sclerosis (MS).[5]

FTY720-P (**2a**) is the first nonnatural agonist of $S1P_1$ to be reported and the bioactive metabolite of fingolimod (**2b**, FTY720),[6] the first oral therapy for relapsing forms of MS (Fig. 1).[7] The efficacy of fingolimod (**2b**) is believed to arise primarily from the agonism of $S1P_1$ by **2a** (h$S1P_1$ RI EC_{50} = 0.0020 μM, 115% efficacy)[3] and the ensuing peripheral lymphocyte depletion.[8]

Notably, fingolimod (**2b**) has also been shown to induce dose-dependent transient bradycardia in preclinical animal models and human subjects.[9] Until recently, the activation of $S1P_3$ by **2a**

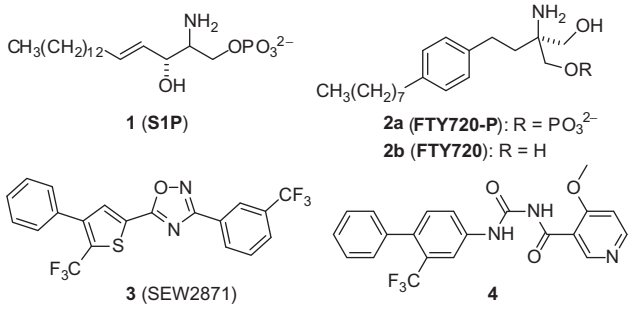

Figure 1. Natural and nonnatural agonists of $S1P_1$.

* Corresponding author. Tel.: +1 805 447 0048; fax: +1 805 480 1337.
E-mail addresses: lewpenn@me.com, lewisp@amgen.com (L.D. Pennington).

0960-894X/$ - see front matter © 2011 Elsevier Ltd. All rights reserved.
doi:10.1016/j.bmcl.2011.10.085

(hS1P$_3$ Ca^{2+} flux EC_{50} = 0.027 μM, 35% efficacy)[10] was believed to be the sole cause of these cardiovascular side effects in humans,[11] and the search for S1P$_3$-sparing synthetic agonists of S1P$_1$ has garnered significant attention.[12] SEW2871 (**3**) is the first example of an S1P$_1$-selective agonist lacking a polar head group that is typical of most synthetic agonists of this receptor (Fig. 1).[13] Although the potency of **3** is modest (hS1P$_1$ RI EC_{50} = 0.27 μM, 86% efficacy),[3] its selectivity for S1P$_1$ versus S1P$_3$ is excellent (hS1P$_3$ Ca^{2+} flux EC_{50} >25 μM).[10,14]

Our laboratory recently disclosed carbamoylnicotinamide **4** as a novel example of this atypical chemotype of S1P$_1$ agonist lacking a polar head group (Fig. 1).[15] Carbamoylnicotinamide **4** displays improved potency (hS1P$_1$ RI EC_{50} = 0.035 μM, 96% efficacy)[3] compared to SEW2871 (**3**), while maintaining excellent selectivity against S1P$_3$ (hS1P$_3$ Ca^{2+} flux EC_{50} >25 μM).[10] The greater cell potency of **4** versus **3** is recapitulated in vivo. Whereas carbamoylnicotinamide **4** effects dramatic reduction of circulating lymphocytes in rat 24 h after a 1 mg/kg oral dose (POC = −78%; $[\mathbf{4}]_{plasma}$ = 63 ng/mL),[15,16] SEW2871 (**3**) requires a much larger dose (30 mg/kg po) to achieve similar levels of peripheral lymphocyte depletion at the 24 h time point (POC = −66%; $[\mathbf{3}]_{plasma}$ = 1100 ng/mL).[16] As part of an effort to discover new and potentially improved atypical chemotypes of S1P$_1$ agonists lacking a polar head group, we set out to explore conformationally constrained analogs of **4**.

Because a large number of heterocyclic bioisosteres of the acyl urea moiety of carbamoylnicotinamide **4** have been reported in S1P$_1$ agonists (e.g., the oxadiazole of **3**),[5,13] we focused our attention on the right-hand side of **4** (Fig. 2). We envisioned replacing the intramolecular hydrogen bond between the carbamoyl NH group and the nicotinamide OMe substituent of **4** with a covalent linkage, and substituting the pyridyl N atom of **4** with a CH group to give quinolinone **5**. This cyclization strategy would simultaneously serve to impart a more rigid conformational constraint and remove a hydrogen bond donor.[17,18] Furthermore, we desired to systematically substitute each CH group in **5** with a N atom to probe the effect on potency and tune molecular and physicochemical properties with minimal impact on molecular weight. This homologous series of aza-substituted, quinolinone-based S1P$_1$ agonists was anticipated to reveal structure–activity relationships (SAR) that might lead to further improvement of in vitro and in vivo activity by the potentially additive effects of multiple N atom substitution. We expected that the synthesis of these aza- and poly-aza-analogs of **5** would challenge this N atom scan (N-scan) SAR strategy.

The results of this study are detailed in Table 1. Pleasingly, quinolinone **5** was found to exhibit similar potency toward S1P$_1$ (hS1P$_1$ RI EC_{50} = 0.070 μM, 110% efficacy)[3] compared to carbamoylnicotinamide **4**. It is also notable that quinolinone **5** is the only compound in Table 1 that displays appreciable agonism of S1P$_3$ (hS1P$_3$ Ca^{2+} flux; **5**: EC_{50} = 1.5 μM, 92% efficacy; **6**–**19**: EC_{50} >2.5 or 25 μM).[10] Other salient features of this investigation are as follows. The data for aza-analogs **7**, **10**, **12**, **13**, **15**, and **16** revealed that N atom substitution at positions 5, 8, 5′, 6′, 3″, and 4″, respectively, has a deleterious effect on potency toward S1P$_1$ (hS1P$_1$ RI EC_{50} = 4.1, 0.19, 1.1, 2.9, 0.31, and 0.45 μM; and 86%, 100%, 59%, 170%, 110%, and 110% efficacy, respectively)[3] compared to **5**. In contrast, the data for aza-analogs **6**, **8**, **9**, **11**, and **14** showed that N atom substitution at positions 2, 6, 7, 3′, and 2″, respectively, has either a beneficial or neutral effect on potency toward S1P$_1$ (hS1P$_1$ RI EC_{50} = 0.041, 0.024, 0.029, 0.042, and 0.060 μM; and 130%, 100%, 120%, 120%, and 110% efficacy, respectively)[3] and, with the exception of the 3′ position (aza-analog **11**), imparts improved cell permeability (P_{app} = 2.3, 5.7, 3.4, <1.0, and 11 × 10^{-6} cm/s, respectively) versus **5**. In general, the effects of a single N atom substitution on solubility and microsomal stability were found to be modest; however, incorporation of a N atom at positions 2″, 3″, or 4″ (compounds **14**, **15**, and **16**, respectively) was observed to improve solubility in 0.010 M aq HCl (Sol = 12, 23, and 6.4 μg/mL, respectively) compared to **5**, and aza-analogs **15** and **16** were the only derivatives found to exhibit >14 μL/min/mg clearance in rat liver microsomes (CL_{int} = 18 and 44 μL/min/mg, respectively).

We desired next to examine the effect of quinolinone **5** and its best aza-analogs **6**, **8**, **9**, **11**, and **14** on peripheral lymphocyte counts (PLC) in vivo (1 mg/kg po).[16] Notably, aza-analog **8** is the only compound that effects statistically significant (P <0.05 versus vehicle by the ANOVA/Dunnett's Multiple Comparison Test) reduction in circulating lymphocytes (POC = −64%; $[\mathbf{8}]_{plasma}$ = 350 ng/mL). Given their comparable in vitro profiles, it is unclear why derivatives **5**, **6**, **9**, **11**, and **14** do not achieve higher plasma levels and realize statistically significant reduction of peripheral lymphocyte counts. Because N atom substitution at positions 3′ and 2″ was shown to have either a beneficial or neutral effect on potency toward S1P$_1$ (compounds **11** and **14**, respectively), diaza-analogs **17** and **18** and triaza-analog **19** were synthesized. The data for diaza-analog **17** showed that N atom substitution at both positions 6 and 3′ has a neutral effect on potency (hS1P$_1$ RI EC_{50} = 0.020 μM, 120% efficacy)[3] and a positive effect on cell permeability (P_{app} = 6.7 × 10^{-6} cm/s) compared to aza-analogs **8** and **11**. In contrast, the data for diaza-analog **18** and triaza-analog **19** revealed that having N atom substitution at both the 6 and 2′ positions has a negative effect on potency (hS1P$_1$ RI EC_{50} = 0.20, 0.21 μM and 100%, 130% efficacy, respectively)[3] but a positive effect on cell permeability (P_{app} = 16 and 15 × 10^{-6} cm/s, respectively) and solubility (Sol = 120, <1.0, 6.7 and >200, 3.0, 5.8 μg/mL, respectively) versus aza-analogs **8** and **14** (for **18**) and diaza-analog **17** (for **19**). Of these three poly-aza-substituted compounds, only diaza-analogs **17** and **18** effect statistically significant (P <0.05 versus vehicle by the ANOVA/Dunnett's Multiple Comparison Test) reduction in circulating lymphocytes (POC = −64% and −32%, respectively; $[\mathbf{17}]_{plasma}$ = 130 ng/mL; $[\mathbf{18}]_{plasma}$ = 150 ng/mL).[16] The data presented in Table 1 show that embedded N atoms are tolerated at specific positions of **5**, and the resulting aza-analogs generally have improved physicochemical properties that can result in markedly enhanced in vivo pharmacodynamics.[19]

Pharmacokinetic profiles of compounds **5**, **8**, and **17** were undertaken in preparation for more detailed studies in vivo (Table 2). In

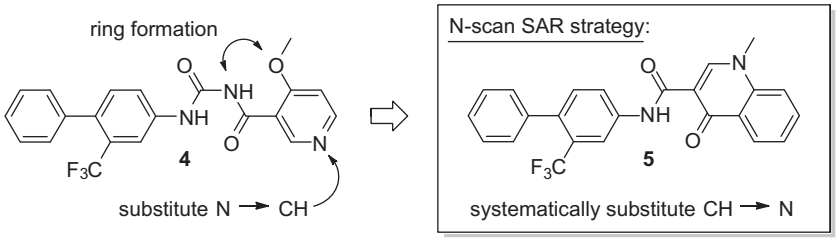

Figure 2. Transformation of **4** → **5** and design of the N-scan SAR strategy.

Table 1
N-scan SAR study of **5**: effects on physicochemical properties, potency, microsomal stability, and lymphocyte count

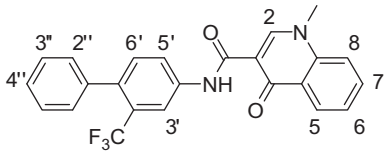

Compd	CH → N	*c*log*P*[a]	ACD log P[b] (ACDLogD$_{7.4}$)	hS1P$_1$ RI EC$_{50}$[c] μM (% eff.)	Sol (μg/mL)[d] HCl, PBS, SIF	P_{app} (ER)[e] (×10^6 cm/s)	CL$_{int}$, RLM[f] (μL/min/mg)	PLC, POC[g] ([C]$_{plasma}$, ng/mL)
5	–	4.8	6.2 (6.2)	0.070 (110)	1.3, <1.0, 11	1.2 (0.40)	<14	–3 (20)[h]
6	2	4.9	5.5 (5.5)	0.041 (130)	<1.0, 1.6, 12	2.3 (1.2)	<14	+6 (9.7)[h]
7	5	3.5	4.7 (4.7)	4.1 (86)	ND[i]	16 (1.4)	<14	ND[i]
8	6	3.5	4.8 (4.8)	0.024 (100)	<1.0, <1.0, 4.9	5.7 (0.80)	<14	–64 (350)[j]
9	7	3.5	4.7 (4.7)	0.029 (120)	<1.0, 2.6, 6.1	3.4 (1.0)	<14	–36 (140)[h]
10	8	3.5	5.3 (5.3)	0.19 (100)	<1.0, <1.0, 5.9	2.2 (1.7)	<14	ND[i]
11	3′	3.8	5.4 (5.4)	0.042 (120)	<1.0, <1.0, 2.3	<1.0 (NR)[k]	<14	+7 (1.3)[h]
12	5′	3.8	5.0 (5.0)	1.1 (59)	ND[i]	<1.0 (NR)[k]	<14	ND[i]
13	6′	4.0	5.8 (5.8)	2.9 (170)	<1.0, <1.0, 13	11 (1.9)	<14	ND[i]
14	2″	3.5	4.8 (4.8)	0.060 (110)	12, <1.0, 5.2	11 (0.80)	<14	+25 (5.1)[h]
15	3″	3.3	4.9 (4.9)	0.31 (110)	23, <1.0, 6.7	18 (1.6)	18	ND[i]
16	4″	3.3	4.8 (4.8)	0.45 (110)	6.4, 7.9, 12	15 (1.5)	44	ND[i]
17	6, 3′	2.4	4.1 (4.0)	0.020 (120)	<1.0, 2.4, 10	6.7 (1.0)	<14	–64 (130)[j]
18	6, 2″	2.2	3.5 (3.5)	0.20 (100)	120, <1.0, 6.7	16 (1.0)	15	–32 (150)[j]
19	6, 3′, 2″	1.2	2.7 (2.7)	0.21 (130)	>200, 3.0, 5.8	15 (1.0)	<14	–32 (140)[h]

[a] Calculated using Daylight Chemical Information Systems software (web site: www.daylight.com).
[b] Calculated using Advanced Chemistry Development (ACD/Labs) software (web site: www.acdlabs.com).
[c] Data represents an average of at least two determinations; see Ref. 15 for experimental details.
[d] Solubility in 0.010 M aqueous hydrogen chloride (HCl), phosphate-buffered saline (PBS) at pH 7.4, or simulated intestinal fluid (SIF).
[e] Apparent permeability (P_{app}) through porcine proximal tubule cells (LLC-PK1 cell line) and efflux ratio (ER).
[f] Estimated intrinsic clearance (CL$_{int}$) determined by incubation of test compound with rat liver microsomes (RLM) for 30 min and measurement of % turnover.
[g] Percent-of-control (POC) reduction versus vehicle in peripheral lymphocyte count (PLC) 24 h after a single oral dose (1 mg/kg; vehicle = 20% Captisol, 1% HPMC, 1% Pluronic F68, pH 2.0 with MSA) administered to female Lewis rats (N = 5/group) and total compound concentration in plasma ([C]$_{plasma}$) at the 24 h time point.
[h] The measured POC reduction in PLC is not statistically significant (P >0.05 versus vehicle by the ANOVA/Dunnett's Multiple Comparison Test).
[i] ND, not determined.
[j] The measured POC reduction in PLC is statistically significant (P <0.05 versus vehicle by the ANOVA/Dunnett's Multiple Comparison Test).
[k] NR, not reportable.

male Sprague–Dawley rats (N = 3) given a single intravenous dose (1 mg/kg), diaza-analog **17** displays a more favorable pharmacokinetic profile (CL = 0.15 L/h/kg, V_{dss} = 5.1 L/kg, $T_{1/2}$ = 24 h) compared to that for both aza-analog **8** (CL = 0.16 L/h/kg, V_{dss} = 9.2 L/kg, $T_{1/2}$ = 41 h) and quinolinone **5** (CL = 0.93 L/h/kg, V_{dss} = 11 L/kg, $T_{1/2}$ = 15 h). Additionally, diaza-analog **17** displays enhanced bioavailability (%F = 60, 95, and 110 for **5**, **8**, and **17**, respectively).[20] Although it is not perfectly linear, diaza-analog **17** also exhibits better dose-proportional exposure at high doses versus **5** and **8** ([AUC$_{0\rightarrow24h}$ (100 mg/kg po)]/[AUC$_{0\rightarrow24h}$ (3 mg/kg po)] = 4.7, 6.0, and 11 for **5**, **8**, and **17**, respectively). The comparable plasma protein binding of **5**, **8**, and **17** (%PPB = 97, 92, and 98, respectively) suggests that the improved pharmacokinetic profile of **17** is not merely the result of greater nonspecific binding in this compartment. Because **17** displays better cell permeability (P_{app} = 6.7 × 10^{-6} cm/s) than carbamoylnicotinamide **4** (P_{app} = 2.3 × 10^{-6} cm/s),[15] and comparable pharmacokinetics,[15] the diminished solubility of **17** (Sol = <1.0, 2.4, 10 μg/mL in HCl, PBS, and SIF, respectively) versus **4** (Sol = 17, 6.6, 16 μg/mL in HCl, PBS, and SIF, respectively)[15] may be responsible for its nonlinear exposure at high doses (⩾100 mg/kg po), a shortcoming that **4** does not suffer.[15]

We next sought to evaluate the pharmacodynamic effects of **5**, **8**, and **17** in more detail (Fig. 3).[16] Following a single oral dose in female Lewis rats (0.30, 1.0, or 3.0 mg/kg), compounds **5**, **8**, and **17** exhibit dose-proportional plasma exposure ([**5**]$_{plasma}$ = 5.5, 18, and 48 ng/mL; [**8**]$_{plasma}$ = 96, 380, and 1100 ng/mL; and [**17**]$_{plasma}$ = 47, 180, and 640 ng/mL, respectively), and concomitant dose-dependent reduction in circulating lymphocytes at the 24 h time point. Statistically significant lymphocyte depletion is first realized for the 3.0 mg/kg dose for **5** and **8** and the 1.0 mg/kg dose for **17** (**5**: –51%, **8**: –64%, and **17**: –67%, respectively; P <0.05, <0.01, and <0.001 versus vehicle by the ANOVA/Dunnett's Multiple Comparison Test, respectively).[21] This dose-dependent decrease in circulating lymphocytes reaching a plateau at 76% maximal reduction (from the 3.0 mg/kg dose of **17**) is consistent with the S1P$_1$ agonist activity of **5**, **8**, and **17**.[13,14]

Compounds **5**, **8**, and **17** were prepared as detailed in Scheme 1, and their syntheses serve to exemplify the general manner in which all of the compounds discussed in Table 1 were synthesized. The preparation of quinolinone **5** was facile. Commercially available compounds 2-(trifluoromethyl)biphenyl-4-amine (**20**) and 1-methyl-4-oxo-1,4-dihydro-3-quinolinecarboxylic acid (**21**) were coupled using *O*-(7-azabenzotriazol-1-yl)-*N*,*N*,*N*′,*N*′-tetramethyluronium hexafluorophosphate (HATU) and Hünig's base to give quinolinone **5** in 62% yield. The synthesis of aza-analog **8** was more demanding. Methylation of commercially available ethyl 4-oxo-1,4-dihydro-1,6-naphthyridine-3-carboxylate (**22**) with Me_2SO_4/K_2CO_3 afforded ethyl 1-methyl-4-oxo-1,4-dihydro-1,6-naphthyridine-3-carboxylate (**23**). Saponification of **23** (LiOH/H_2O) provided lithium carboxylate **24**, which was used in the next step of the synthesis without purification. The union of biphenylamine **20** and **24** was mediated by HATU/*i*-Pr$_2$NEt to afford aza-analog **8** in 30% yield. The synthesis of diaza-analog **17** was the most challenging of these three compounds. Commercially available 6-(trifluoromethyl)-2-pyridinamine (**26**) was regioselectively brominated using NBS in $CHCl_3$ to give 5-bromo-6-(trifluoromethyl)-2-pyridinamine (**27**) in moderate yield. A phenyl group was appended to **27** by palladium-mediated cross-coupling ($(Ph_3P)_4Pd/K_2CO_3$) with phenylboronic acid, affording 5-phenyl-6-(trifluoromethyl)-2-pyridinamine (**28**) in 84% yield. The lower nucleophilicity of pyridinamine **28** versus biphenylamine **20** demanded recourse to more forcing coupling conditions than those used for the synthesis of **5**

Table 2
Pharmacokinetic profiles of **5**, **8**, and **17**[a]

Compd	PPB (%)[b] rat	CL (L/h/kg)[c] 1 mg/kg iv	V_{dss} (L/kg)[c] 1 mg/kg iv	$T_{1/2}$ (h)[c] 1 mg/kg iv	$AUC_{0\rightarrow 24h}$ (ng h/mL)[d] 3 mg/kg po	F[e] (%)	$AUC_{0\rightarrow 24h}$ (ng h/mL)[f] 100 mg/kg po
5	97	0.93	11	15	1200	60	5800
8	92	0.16	9.2	41	5100	95	31000
17	98	0.15	5.1	24	12000	110	130000

[a] In vivo experiments were conducted using male Sprague–Dawley rats (N = 3/group).
[b] Percent rat plasma protein binding (PPB) measured in vitro following separation by ultracentrifugation.
[c] Clearance (CL), volume of distribution (V_{dss}), and half-life ($T_{1/2}$) determined following a single intravenous dose (1 mg/kg; vehicle = DMSO).
[d] Area under the plasma concentration–time curve ($AUC_{0\rightarrow 24\ h}$) determined following a single oral dose (3 mg/kg; vehicle = 20% Captisol, 1% HPMC, 1% pluronic F68, pH 2.0, with MSA).
[e] Percent bioavailability (F) calculated using $AUC_{0\rightarrow\infty}$ values determined from the 1 mg/kg iv and 3 mg/kg po doses.
[f] Area under the plasma concentration–time curve ($AUC_{0\rightarrow 24\ h}$) determined following a single oral dose (100 mg/kg; vehicle = 20% Captisol, 1% HPMC, 1% pluronic F68, pH 2.0, with MSA).

and **8**. Lithium carboxylate **24** was treated with $SOCl_2$ in toluene at reflux to provide acid chloride **25** (quantitative yield, crude). Finally, exposure of a solution of **25** and **28** in dichloroethane to DMAP/*i*-Pr_2NEt afforded diaza-analog **17** in 63% yield. Comparison of the synthesis of compounds **5**, **8**, and **17** illustrates that incorporating an increasing number of specifically placed N atoms into a scaffold often results in progressively more lengthy and complex synthetic sequences.

In conclusion, a set of conformationally constrained, atypical chemotypes of $S1P_1$ agonists lacking a polar head group was discovered. This homologous series of aza-substituted, quinolinone-based agonists of $S1P_1$ provided insight into SAR trends that allowed improvement of both in vitro and in vivo activity. This study illustrates that the conceptually simple N-scan SAR strategy of systematically incorporating N atoms into a scaffold to tune molecular and physicochemical properties can lead to significant improvement in potency, selectivity, pharmacokinetics, and pharmacodynamics (e.g., quinolinone **5** → aza-analog **8** → diaza-analog **17**). However, this approach can be rendered challenging by the progressively more complex synthesis of these aza-substituted compounds. Finally, although diaza-analog **17** displays improved pharmacokinetics and pharmacodynamics compared to quinolinone **5** and aza-analog **8**, it exhibits nonlinear exposure at high doses required to establish a safety margin ($\geqslant$100 mg/kg po), limiting the prospects for further development of this compound.

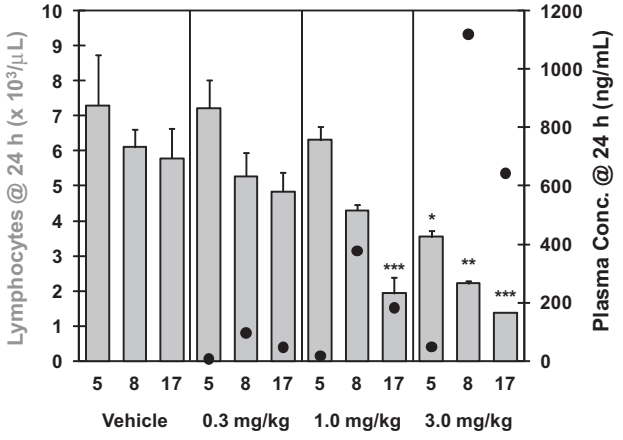

Figure 3. Female Lewis rats (N = 5/group; vehicle = 20% Captisol or HPBCD, 1% HPMC, 1% Pluronic F68, pH 2.0 with MSA) administered a single oral dose of **5**, **8**, or **17** (0.30, 1.0, or 3.0 mg/kg) showed dose-proportional plasma exposure (black circles represent average plasma concentration ± SE) and dose-dependent reduction in circulating lymphocytes (gray bars represent average blood lymphocyte counts ± SE) at the 24 h time point (statistical significance: $^{*}P$ <0.05, $^{**}P$ <0.01, or $^{***}P$ <0.001 versus vehicle by the ANOVA/Dunnett's Multiple Comparison Test); see Ref. 15 for experimental details.

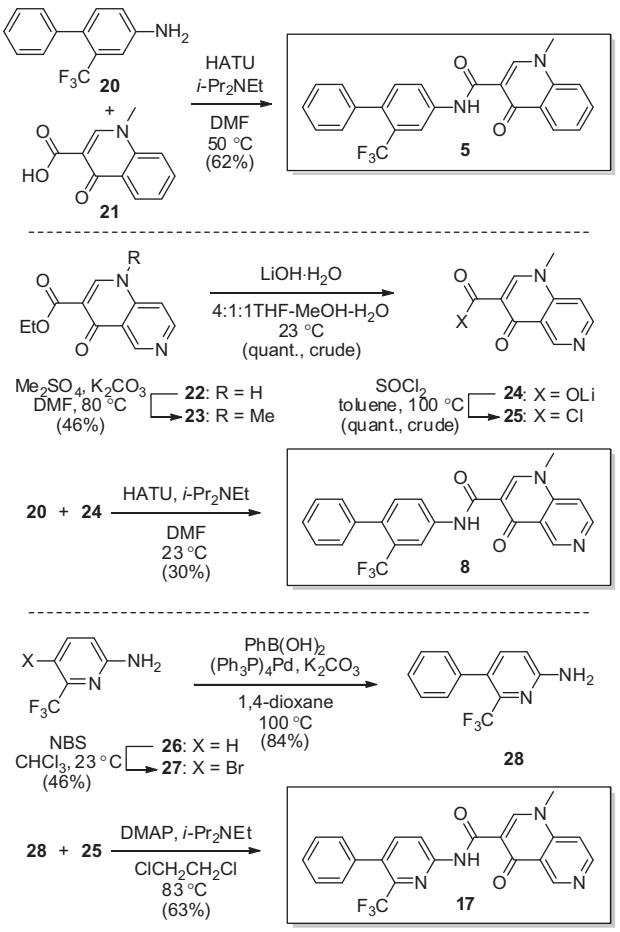

Scheme 1. Chemical synthesis of compounds **5**, **8**, and **17**.

Efforts to modify the aza-quinolinone scaffold to overcome this challenge are the subject of a future disclosure.

Acknowledgments

We thank Valerie Almon, Ronya Primack, and Elizabeth Tominey (Pharmacokinetics and Drug Metabolism, Amgen) for in vivo pharmacokinetic studies. All live animal studies were conducted in an AAALAC-accredited facility and husbandry procedures met all of the recommendations of the Guide for the Care and Use of Laboratory Animals. All work using research animals was conducted under Institutional Animal Care and Use Committee (IACUC) approved protocols.

References and notes

1. For a review, see: Rosen, H.; Gonzalez-Cabrera, P. J.; Sanna, M. G.; Brown, S. *Annu. Rev. Biochem.* **2009**, *78*, 743.
2. For a review, see: Cyster, J. G. *Annu. Rev. Immunol.* **2005**, *23*, 127.
3. By measurement of RI of an $hS1P_1$–eGFP fusion protein in U2OS cells (% efficacy is reported relative to known $hS1P_1$ agonist 1-(4-(6-benzylbenzofuran-2-yl)-3-fluorobenzyl)azetidine-3-carboxylic acid at a concentration of 1.0 μM); see: Cee, V. J.; Frohn, M.; Lanman, B. A.; Golden, J.; Muller, K.; Neira, S.; Pickrell, A.; Arnett, H.; Buys, J.; Gore, A.; Fiorino, M.; Horner, M.; Itano, A.; Lee, M. R.; McElvain, M.; Middleton, S.; Schrag, M.; Rivenzon-Segal, D.; Vargas, H. M.; Xu, H.; Xu, Y.; Zhang, X.; Siu, J.; Wong, M.; Bürli, R. W. *ACS Med. Chem. Lett.* **2011**, *2*, 107. and Ref. 15 for experimental details.
4. For a review, see: Rivera, J.; Proia, R. L.; Olivera, A. *Nat. Rev. Immunol.* **2008**, *8*, 753.
5. For a review, see: Bolli, M. H.; Lescop, C.; Nayler, O. *Curr. Top. Med. Chem.* **2011**, *11*, 726.
6. Albert, R.; Hinterding, K.; Brinkmann, V.; Guerini, D.; Müller-Hartwieg, C.; Knecht, H.; Simeon, C.; Streiff, M.; Wagner, T.; Welzenbach, K.; Zécri, F.; Zollinger, M.; Cooke, N.; Francotte, E. *J. Med. Chem.* **2005**, *48*, 5373.
7. Kappos, L.; Radue, E.-W.; O'Connor, P.; Polman, C.; Hohlfeld, R.; Calabresi, P.; Selmaj, K.; Agoropoulou, C.; Leyk, M.; Zhang-Auberson, L.; Burtin, P. *N. Engl. J. Med.* **2010**, *362*, 387.
8. Mandala, S.; Hajdu, R.; Bergstrom, J.; Quackenbush, E.; Xie, J.; Milligan, J.; Thornton, R.; Shei, G.-J.; Card, D.; Keohane, C.; Rosenbach, M.; Hale, J.; Lynch, C. L.; Rupprecht, K.; Parsons, W.; Rosen, H. *Science* **2002**, *296*, 346.
9. Schmouder, R.; Serra, D.; Wang, Y.; Kovarik, J. M.; DiMarco, J.; Hunt, T. L.; Bastien, M.-C. *J. Clin. Pharmacol.* **2006**, *46*, 895. and references cited therein.
10. By measurement of Ca^{2+} mobilization in CHO-K1 cells ex-pressing $hS1P_3$ and a chimeric $G_{q/i5}$ G-protein (% efficacy is reported relative to S1P at a concentration of 0.20 μM; >[highest concentration tested] is reported for compounds that do not achieve >10% of control activity); see Ref. 15 for experimental details.
11. Hamada, M.; Nakamura, M.; Kiuchi, M.; Marukawa, K.; Tomatsu, A.; Shimano, K.; Sato, N.; Sugahara, K.; Asayama, M.; Takagi, K.; Adachi, K. *J. Med. Chem.* **2010**, *53*, 3154.
12. Lanman, B. A.; Cee, V. J.; Cheruku, S. R.; Frohn, M.; Golden, J.; Lin, J.; Lobera, M.; Marantz, Y.; Muller, K. M.; Neira, S. C.; Pickrell, A. J.; Rivenzon-Segal, D.; Schutz, N.; Sharadendu, A.; Yu, X.; Zhang, Z.; Buys, J.; Fiorino, M.; Gore, A.; Horner, M.; Itano, A.; McElvain, M.; Middleton, S.; Schrag, M.; Vargas, H. M.; Xu, H.; Xu, Y.; Zhang, X.; Siu, J.; Bürli, R. W. *ACS Med. Chem. Lett.* **2011**, *2*, 102. and references cited therein.
13. Hale, J. J.; Lynch, C. L.; Neway, W.; Mills, S. G.; Hajdu, R.; Keohane, C. A.; Rosenbach, M. J.; Milligan, J. A.; Shei, G.-J.; Parent, S. A.; Chrebet, G.; Bergstrom, J.; Card, D.; Ferrer, M.; Hodder, P.; Strulovici, B.; Rosen, H.; Mandala, S. *J. Med. Chem.* **2004**, *47*, 6662.
14. Sanna, M. G.; Liao, J.; Jo, E.; Alfonso, C.; Ahn, M.-Y.; Peterson, M. S.; Webb, B.; Lefebvre, S.; Chun, J.; Gray, N.; Rosen, H. *J. Biol. Chem.* **2004**, *279*, 13839. $S1P_1$ agonists have been shown to effect ~70% maximal reduction in circulating lymphocytes; see Ref. 13.
15. Pennington, L. D.; Sham, K. K. C.; Pickrell, A. J.; Harrington, P. E.; Frohn, M. J.; Lanman, B. A.; Reed, A. B.; Croghan, M. D.; Lee, M. R.; Xu, H.; McElvain, M.; Xu, Y.; Zhang, X.; Fiorino, M.; Horner, M.; Morrison, H. G.; Arnett, H. A.; Fotsch, C.; Wong, M.; Cee, V. J. *ACS Med. Chem. Lett.* **2011**, *2*, 752.
16. Female Lewis rats ($N = 5$/group) were administered a single oral dose of each compound; after 24 h, lymphocyte counts in blood and compound concentrations in plasma were measured (the 24 h time point was selected for these studies, as it was found to mitigate the effects of dosing on lymphocyte counts; see Ref. 15 for experimental details).
17. For a review, see: Hitchcock, S. A.; Pennington, L. D. *J. Med. Chem.* **2006**, *49*, 7559.
18. For a review, see: Ursu, O.; Rayan, A.; Goldblum, A.; Oprea, T. I. *WIREs Comp. Mol. Sci.* **2011**, *1*, 760.
19. Comparison of the ACDLogP and $ACDLogD_{7.4}$ values for each compound in Table 1 indicates that all are calculated to be neutral at physiological pH, and analysis of the ACD$\log P$ and $c\log P$ values reveals that each CH → N substitution typically effects ~1 unit reduction in calculated $\log P$.
20. Calculated using the $AUC_{0\rightarrow\infty}$ values determined from the 1 mg/kg iv and 3 mg/kg po doses.
21. For aza-analog **8**, the higher dose required to achieve statistically significant reduction in circulating lymphocytes in the dose–response study (3.0 mg/kg po; Fig. 3) versus the single dose experiment (1 mg/kg po; Table 1) may arise from the lower peripheral lymphocyte counts and greater variability in the vehicle group for this study ($6.1 \pm 2.5 \times 10^3/\mu L$ vs $8.4 \pm 1.5 \times 10^3/\mu L$, respectively), as the peripheral lymphocyte counts and variability ($4.3 \pm 0.84 \times 10^3/\mu L$ vs $3.1 \pm 1.2 \times 10^3/\mu L$, respectively), as well as total compound concentration in plasma and variability (380 ± 55 ng/mL vs 350 ± 23 ng/mL) were similar for the 1.0 mg/kg po dose in both studies.